ELSEVIER

Biochimica et Biophysica Acta 1479 (2000) 123–134

BIOCHIMICA ET BIOPHYSICA ACTA
BBA

www.elsevier.com/locate/bba

Interactions between subdomains in the partially folded state of staphylococcal nuclease

Keqiong Ye, Guozhong Jing, Jinfeng Wang *

National Laboratory of Biomacromolecules, Institute of Biophysics, Chinese Academy of Sciences, 15 Datun Road, Beijing 100101, China

Received 29 November 1999; received in revised form 4 March 2000; accepted 17 March 2000

Abstract

Staphylococcal nuclease can be roughly divided into a β-subdomain in N-terminal and an α-subdomain in C-terminal. They fold sequentially under certain conditions, causing a partially folded intermediate state in which the native-like β-barrel persists while α-helix regions largely disorder. To investigate the possible long-range interactions between the two subdomains in the intermediate, N-terminal fragments have been used as intermediate analogues, with polypeptide ending at positions 102, 110, 121 and 135 and with a tryptophan substitution at position 66 or 88 to facilitate the observation of the β-barrel. Segment-resolved interactions between β-barrel and residues 103–135 were identified by comparing their spectroscopic properties of fluorescence, circular dichroism and NMR and by their stability. Except for unstable V66W102, the guanidine and thermal denaturation of fragments are cooperative and well approximated by the two-state transition. Minimal stable structure units of both tryptophan-containing fragments comprise residues 1–110. With the main interaction in segment 103–135, residues 103–110 contribute approximate 2 kcal/mol to the stability. Elongation of C-terminal from 110 residue neither increases the stability nor alters the structure core of the G88W fragments. However, residues 111–121 influence the tertiary structure of the V66W fragments suggesting its minor interactions with β-barrel.

Keywords: Staphylococcal nuclease; Fragment; Tryptophan mutation; Protein stability; Intermediate state; Subdomain

1. Introduction

The mechanisms by which proteins fold to a native state remain a challenging question for biologists [1]. The structure and dynamics of folding intermediates have long been of interest because of the relevance of their conformations to the protein folding pathways. Folding intermediates with varied structure content have been identified [2,3]. It has been suggested that one kind of folding intermediate consists of folding units or folding subdomains which are cooperatively formed structural regions that form independently of other regions in proteins [4]. The sequential folding of individual subdomains has

Abbreviations: SNase, staphylococcal nuclease; CD, circular dichroism; GuHCl, guanidine hydrochloride; NMR, nuclear magnetic resonance; pdTp, 3′,5′-bisphospho-2′-deoxythymidine; V66W135, The N-terminal fragments of staphylococcal nuclease are designated by the mutation it contains followed by the length of the polypeptide chain. For example, V66W135 stands for the fragment where Val-66 is replaced by Trp and contains residue 1–135. WT149 refers to wild-type SNase containing the full-length 149 residues

* Corresponding author. Fax: +86-10-6487-2026;
E-mail: jfw@sun5.ibp.ac.cn

0167-4838/00/$ – see front matter
PII: S0167-4838(00)00060-1

revealed the modular nature in several small single-domain proteins [5–7].

Staphylococcal nuclease (SNase), a small globular protein (149 residues) with a five-stranded β-barrel and three α-helices (Fig. 1), folds efficiently and reversibly and has been investigated extensively as a folding model [7–27]. Thermodynamically, it behaves as a cooperative unit and the equilibrium unfolding transition fits a two-state model well. However, in acidic condition or after some *m*−mutations, SNase unfolds via a three-state mechanism as revealed by differential scanning calorimetry studies [7–8]. Pulsed hydrogen exchange and NMR methods showed an early protection of hydrogen in part of the β-barrel indicating that the β-barrel is the first formed structure unit in SNase [10]. Kinetic folding and unfolding studies of a proline-free SNase also revealed a folding intermediate which is consistent with a partially folded state having a stable β-barrel and a largely disordered α-helical region [11]. These suggest that the structure of SNase can be split into two subdomains, with predominantly α-helix and β-sheet, respectively. The folding intermediates are results of sequential folding or unfolding of two subdomains. The β-subdomain which has better stability and independence, constitutes the main structured part of the intermediate [4,7–9]. Two interesting questions are to be addressed here. The first is whether the α-subdomain in the intermediate, which is less structured or disordered, has long-range interactions with the more structured β-subdomain and to what extent the interactions affect the stability of the β-subdomain. The second is whether a single cooperatively structured β-subdomain can be isolated from the modular SNase. The isolated subdomain would have a simpler fold module compared with the full-length SNase and be amenable to further study.

These two questions have been investigated using a protein dissection method. A 1–136 fragment of SNase lacking the 13 C-terminal residues in the physiological condition displayed structural features very similar to the intermediate state with native-like β-barrel and little α-helix content [12–17]. Taking the N-terminal fragment as an intermediate analogue, the partially folded fragment 1–136 was cut from the C-terminal to observe the change on the structure and stability. If one deleted (or added) segment is completed disordered, it should make no net contribution to the stability of the resulting structure. Four fragments containing 1–102, 1–110, 1–121 and 1–135 residues were prepared, with a tryptophan mutation at position 66 or 88. These N-terminal fragments differ in the residues which roughly form a secondary structure unit in the native state of SNase (see Fig. 1), namely helix 2 (98–106), the loop linking helix 2 and 3 (107–120) and helix 3 (121–135) [18–19]. The tryptophan mutations were introduced for two reasons. First, they are used as a structure probe located at the β-barrel. These fragments have only one Trp residue at the β-barrel since the tryptophan at position 140 in full-length SNase is deleted from the fragments. Secondly, mutations V66W and G88W have both been shown to stabilize the intermediate state in full-length SNase [7,8]. Furthermore, fragments of V66W136 and G88W136 have been previously found to have a cooperative structured core in the β-barrel and their thermodynamic and spectroscopic properties approach the unfolding intermediate state of V66W149 and G88W149 [16,17]. So the V66W and G88W N-terminal fragments are well suited as a model for exploring the role of long-range interactions between the C-terminal α-subdomain and the N-terminal β-barrel subdomain in the stability of the intermediate state.

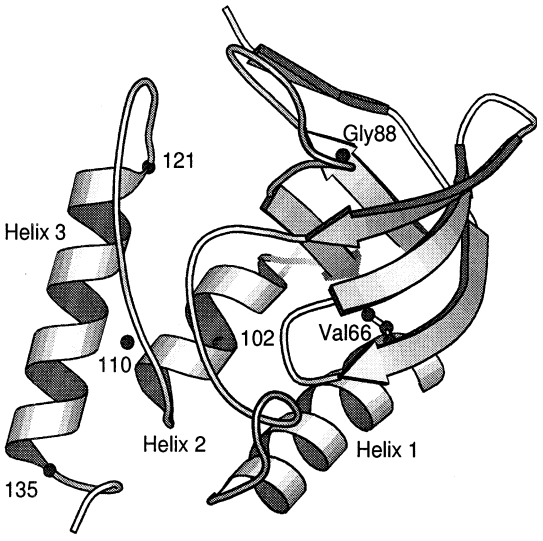

Fig. 1. Ribbon diagram of staphylococcal nuclease, based on the crystal structure (PDB entry 1stn). The side chain of Val-66 and Gly-88 (mutation sites) are shown explicitly. The ending residues of four N-terminal fragments 1–102, 1–110, 1–121, and 1–135 are marked. Three helices are labeled. The diagram was prepared using the program MOLSCRIPT [36].

This study investigates the state of V66W- and G88W fragments by CD, fluorescence and NMR and obtains qualitative thermodynamic parameters from GuHCl and thermal induced denaturation. Residues 103–110 contribute the largest increase of stability to the partially folded fragments. Fragments of V66W110 and G88W110 are shown to be stable isolated subdomains.

2. Materials and methods

2.1. Plasmid construction, protein expression and purification

The single-position mutants V66W and G88W were produced by the polymerase chain reaction in the gene of wild-type SNase (originally provided by Dr. Davis Shortle) and have been confirmed by sequencing. Wild-type fragment genes containing stop code TAA at 103, 111, 122, and 136 have been constructed in this laboratory [25]. The tryptophan-containing fragment genes were constructed by ligating the N-terminal part of tryptophan-containing genes with the C-terminal part of fragment genes at an internal *Hin*dIII site in residue 102. All genes were cloned in plasmid pET-3d and expressed in the BL21(DE3) strain of *Escherichia coli* [28]. Gene manipulations followed standard protocols [29].

Protein expression was induced in LB culture with 0.4 mM isopropyl-β-thiogalactose (IPTG) when the A_{600} of the culture reached values of 0.6–1.0. After an additional 3–4 h of incubation at 37°C, the cells were collected by centrifugation and suspended per gram wet weight of cells in 4 ml lysis buffer containing 50 mM Tris–HCl, pH 9.2, 2mM EDTA, 2% Triton X-100 and 0.5 mM freshly added phenylmethylsulfonylfluoride (PMSF). Cells were lysed by sonication and centrifuged at $22\,000\times g$ for 15 min at 4°C. Since these fragments were expressed largely as inclusion bodies, the supernatants containing most of soluble protein were discarded. The top layer of the pellet (membrane) was then carefully washed away. The resulting pellet (inclusion body plus cell debris) was resuspended in lysis buffer by short sonicating and spun at $22\,000\times g$ at 4°C for 15 min. After repeating the wash procedure two times, the inclusion body in the pellet was dissolved in loading buffer containing 50 mM Tris–HCl, pH 9.2 and 6 M urea. After centrifugation, the supernatant was loaded onto a CM-25 carboxymethyl-Sephadex column pre-equilibrated with the loading buffer, and then the protein was eluted in the same buffer with 0.5 M NaCl. The main peak was pooled, dialyzed extensively against water, and then lyophilizated. The protein was further purified by dissolving in 10 mM Tris–HCl, pH 7.0, 0.1 M NaCl and loaded onto a Sepharose-12 size exclusive column. The main peak was collected and used in experiments directly. The purity of samples were checked by SDS–PAGE to be $>95\%$.

The protein concentration was determined by UV absorbance at 280 nm using the published molar extinction coefficients of 15 600 M^{-1} cm^{-1} for WT149, calculated coefficients of 14 650 M^{-1} cm^{-1} for V66W121, G88W121, V66W135 and G88W135 and 12090 M^{-1} cm^{-1} for V66W110, G88W110, V66W102 and G88W102 by the method of Gill and von Hippel [30].

2.2. CD and fluorescence measurements

CD spectra were measured on a Jasco 720 spectropolarimeter at 20°C. Data were recorded over the ranges of 260–320 nm and 190–260 nm with 1-cm and 0.01-cm path lengths, respectively. Measurements were acquired in 1-nm increments with an integration time of 2 s for the far-UV region and 4 s for aromatic region. Typically, six scans were averaged for each measurement. The samples were at concentrations of 50–100 μM in 10 mM Tris–HCl (pH 7.0) and 0.1 M NaCl buffer for both spectral measurements. For the GuHCl denaturation study, samples of 3–5 μM were placed in a 1×1 cm cuvette with a small magnetic stir bar in the bottom for mixing and the ellipticity at 222 nm was recorded as the 30-s average of the signal.

The fluorescence intensity measurements were performed on a Hitachi F4010 spectrofluorometer. Samples were excited at 295 nm and the emission was recorded at 325 nm. The excitation and emission band widths were both 10 nm. The emission spectrum were collected on a Hitachi F4500 spectrofluorometer at 295 nm with excitation and emission band widths of 5 and 2.5 nm, respectively. The sample

temperature was maintained at 20°C by a water-jacketed cuvette holder.

In the GuHCl-induced unfolding and acrylamide quenching experiments, aliquots of 8 M guanidine hydrochloride (Ultrapure from Sigma) or 8 M acrylamide (recrystallized from ethyl acetate) were added to a 2-ml sample of 3–5 μM protein in a 1-cm path length quartz fluorescence cuvette. The solution was vigorously mixed by a magnetic stirring bar inside the cuvette. The fluorescence signal was recorded when equilibrium was reached (5 min required in the transition zone of WT149, but fairly short for the fragments).

In thermal unfolding experiments, the sample temperature was controlled by a circulating water bath and was monitored directly by a Model 305 thermometer with a K-type thermocouple, which had been calibrated against an ice/water mixture as 0.0°C just before the experiments. The heating rate was 0.5°C/min and the cooling rate was 1.0°C/min. For each sample in a stopped cuvette, two sets of fluorescence data were collected during heating from 10 to 76°C and cooling to 10°C. The two sets of data were analyzed separately.

2.3. Nuclear magnetic resonance spectroscopy

The proteins were dissolved in 90% H_2O/10% D_2O and 50 mM d4-acetate buffer at pH 4.9. For V66W102 and G88W102, the sample concentration was 50 μM to alleviate aggregation. Others were at concentrations of 1 mM. ^{1}H-NMR spectroscopy was performed at 600.1 MHz on a Bruker DMX spectrometer. One-dimensional ^{1}H spectra were acquired at 20°C using a spectral width of 20 ppm, 8 K complex points, and a recycle delay of 1.5 s with 128 transients for 1 mM samples and 6-K transitions for 50 μM samples, processed with 1 Hz exponential line broadening. The water suppression was achieved using WATERGATE [32]. Chemical shifts were referenced to 0 ppm with internal 2,2-dimethyl-2-silapentane-5-sulfonic acid (DSS).

2.4. Data analysis of quenching experiments

Fluorescence intensities were corrected for any dilution effects and for acrylamide absorbance at the excitation wavelength. Then the quenching data was fitted by the modified Stern–Volmer equation taking into account not only dynamic, but also static quenching [31]:

$$F_0/F = (1 + K_{sv}[Q])\exp(V[Q]) \quad (1)$$

where F_0 and F are the fluorescence intensities in the absence and presence of quencher, K_{sv} and V are the dynamic and static quenching constants, and $[Q]$ is the total quencher concentration. Due to uncertainty in separating the static V and dynamic K_{sv} components, the sum of K_{sv} and V (which is also equal to the initial slope of a Stern–Volmer plot) were reported as the effective quenching constant, $K_{sv,eff}$ [17].

2.5. Data analysis of unfolding reaction

After subtracting the blank signal and corrected for dilution, the GuHCl denaturation data was evaluated based on the two-state and linear extrapolation models [33]

$$I = [(I_n + m_n[D]) + (I_u + m_u[D])\exp(-\Delta G'/RT)]/ [1 + \exp(-\Delta G'/RT)] \quad (2)$$

$$\Delta G' = \Delta G^\circ H_2O + m[D] \quad (3)$$

where I is the fluorescence intensity or ellipticity. The linear baselines of pre- and post-transition regions are assumed: I_n and I_u are the intrinsic signals of the native and unfolded states in the absence of denaturant, m_n and m_u are constants that represent the dependence of the signals on the denaturant concentration $[D]$ in native and unfolded states. $\Delta G'$ is the free energy of unfolding at a given denaturant concentration which is assumed to be linear according to Eq. 3. $\Delta G^\circ H_2O$ is the free energy change for unfolding in the absence of denaturant, and m describes the dependence of the free energy change on denaturant concentration. R is the ideal gas constant. T is the absolute temperature in Kelvin.

The thermal denaturation data was analyzed using the two-state model along with the van 't Hoff equation:

$$I = [(I_n + m_n T) + (I_u + m_u T)\exp(-\Delta G'/RT)]/ [1 + \exp(-\Delta G'/RT)] \quad (4)$$

$$\Delta G' = \Delta H^{\circ}_{m,un}(1-T/T_m)$$

$$-\Delta C_p[T_m - T + T\ln(T/T_m)] \quad (5)$$

The meanings of the letters in Eq. 4 are the same as in Eq. 2 except that m_n and m_u represent the temperature dependence of the pure signal and $\Delta G'$ is the free energy of unfolding at a specific temperature T. In Eq. 5, $\Delta H^{\circ}_{m,un}$ is the enthalpy change for the transition at the transition temperature T_m and ΔC_p is the heat capacity difference between folded and unfolded protein which is assumed to be independent of temperature.

The fluorescence and CD data of GuHCl denaturation were fitted to Eqs. 2 and 3 while the fluorescence data of thermal denaturation was fitted to Eqs. 4 and 5. The non-linear least-squares fit was done using the Levenberg–Marquardt algorithm in Origin 5.0 (Microcal Software), usually with all parameters floating (I_n, I_u, m_n, m_u, $\Delta G^{\circ}H_2O$, m or $\Delta H^{\circ}_{m,un}$, T_m and ΔC_p). Most fits completed successfully except for the thermal unfolding data of G88W102. The I_n and I_u at 20°C of G88W102 were arbitrarily fixed in fitting as values from the GuHCl denaturation results for G88W102. The reported errors were estimated from the repeated experiments of some samples. The errors directly from fitting routine were usually smaller than the estimated uncertainties. The unfolded state fraction was determined using I, I_n, I_u, m_n, and m_u. V66W102 is an unstable fragment, largely denatured at zero GuHCl. Its stability was estimated using ammonium sulfate renaturation according to Shortle et al.'s method [21].

3. Results

3.1. Secondary structure: far-UV CD spectra

Size exclusion column experiments showed that the two shortest fragments, V66W102 and G88W102, exhibited a strong tendency to associate at high protein concentrations. Though aggregation could not be ruled out at a concentration of 50 μM for V66W110 and G88W102, the extent of aggregation is small since nearly the same far-UV CD spectra were obtained at one-tenth of this concentration with a 10-fold greater path length. For the other fragments, little to no dependence of the elution volume on protein concentration (0.02–1 mM) was found indicating no aggregation (data not shown). In addition, they had good NMR spectra at a concentration of 1 mM.

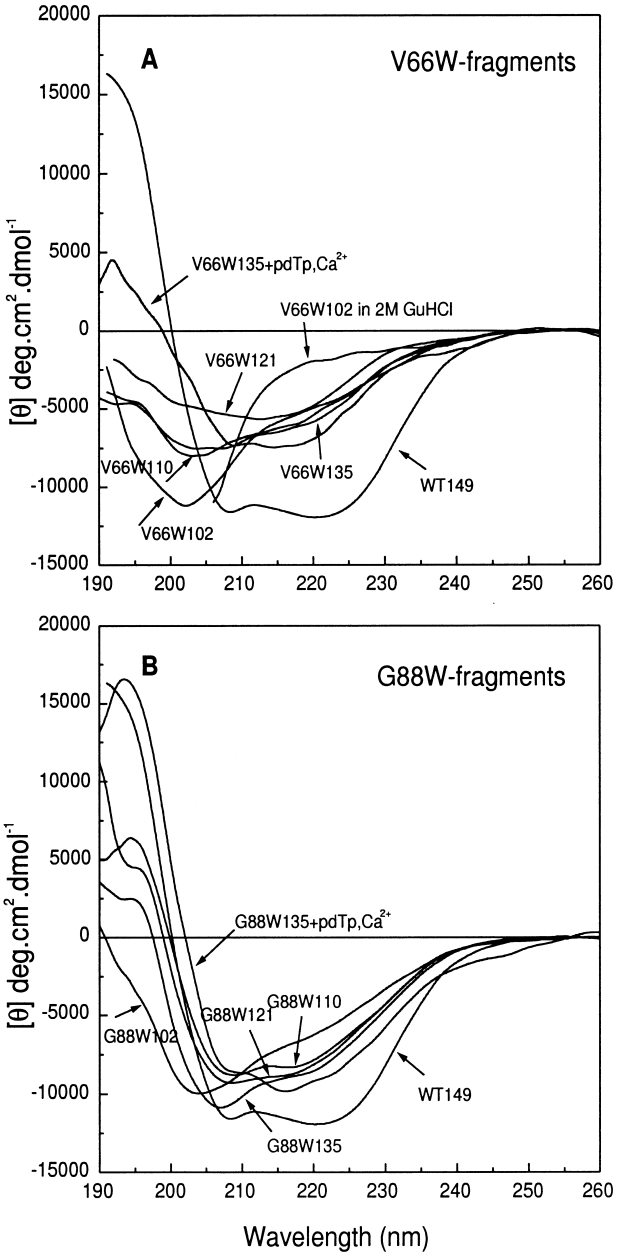

Fig. 2. Circular dichroism spectra in far-UV region measured for (A) V66W fragments and (B) G88W fragments. The full-length nuclease is shown for comparison. Proteins concentration were 50–100 μM in 0.1 M NaCl/10 mM Tris–HCl/pH 7.0 at 20°C. Ligand binding was done by adding 2 mM pdTp and 10 mM Ca^{2+}. G88W fragments show more α-helix features than the corresponding V66W fragments.

The far-UV CD spectra, Fig. 2A,B, were used to assess the secondary structure, especially the α-helix element. The deconvolution results obtained using SELCON3 [34] are listed in Table 1. Interestingly, while the α-helical content varies widely in the fragments, the β-sheet content differences are relatively small all with similar content to the full-length SNase. Generally, the G88W fragments display more helical component than the corresponding V66W fragments. Upon addition of SNase ligands Ca^{2+} and pdTp, both of the 1–135 fragments shift to native-like state. G88W135 is more capable of restoring the native state with ligand binding.

V66W102 shows many features of unstructured elements, with a minimum around 202 nm close to the random coil peak at 197 nm. However, upon addition of denaturant GuHCl, the ellipticity at 210–220 nm was reduced indicating that the residual structure in V66W102 was probably broken down by the denaturant.

Table 1
Estimated secondary structure contents and fluorescence parameters of staphylococcal nuclease fragments[a]

Fragments	α[b]	β[b]	T[b]	λ^{c}_{max} (nm)	$K^{d}_{sv,eff}$ (M^{-1})
WT149	47	27	32	335.9	4.36
V66W135	10	26	18	327.9	2.05
V66W121	9	30	21	327.4	2.11
V66W110	10	20	15	329.9	2.34
V66W102	7	17	13	338.6	5.12
G88W135	31	24	35	340.5	6.52
G88W121	24	31	25	341.1	6.54
G88W110	21	27	23	340.0	6.47
G88W102	13	17	14	342.0	6.89
Denatured[e]				350.9	8.11

[a]Protein concentrations were 3 μM in 10 mM Tris–HCl/pH 7.0/0.1 M NaCl in all fluorescence experiments.
[b]The secondary structures were estimated by deconvoluting CD spectra using the program SELCON3 with a 37-protein reference data set (including five denatured proteins). (http://lamar.colostate.edu/~sreeram/SELCON3/). The α content includes the regular and distorted helix and the β content includes the regular and distorted sheet. T stands for turn. The residue numbers are shown.
[c]The error in emission maximum is less than ±1 nm.
[d]Acrylamide quenching constant from fitting of Eq. 1. $K_{sv,eff}$ is the sum of K_{sv} and V. Estimated average error in $K_{sv,eff}$ is less than ±5%.
[e]V66W102 in the presence of 2 M GuHCl.

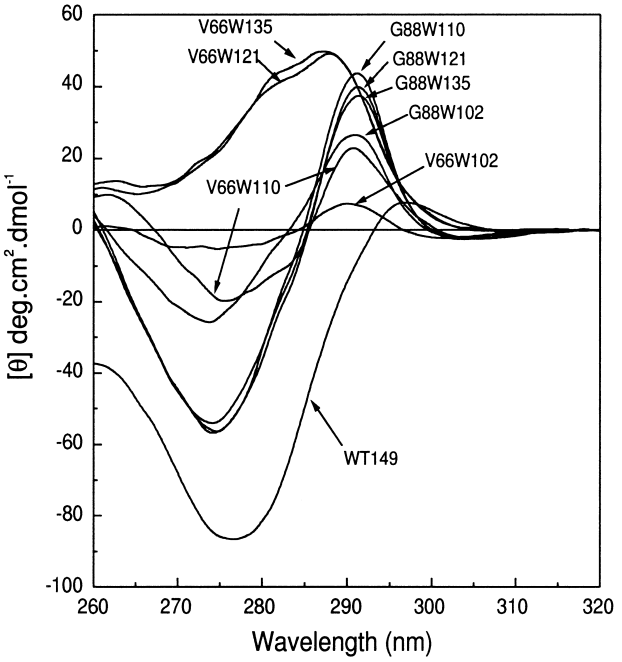

Fig. 3. Circular dichroism spectra in near-UV region measured for nuclease fragments. Conditions are the same as in Fig. 2. Note the significant change between V66W121 and V66W110.

3.2. Tertiary structure: near-UV CD, 1D-NMR, and tryptophan fluorescence

Fig. 3 shows the near-UV CD spectra which report the asymmetry of aromatic amino acid environment. Except for V66W102, all fragments displayed pronounced CD signals in the near-UV region, which has often been taken as representing the existence of tertiary structures in proteins. The different tryptophan positions cause the WT149, V66W and G88W fragments to have quite different profiles. The very similar spectra for all G88W fragments, except for reduced intensity for G88W102, suggest similar tertiary packing in the rigid part of their structure. The spectra of V66W135 and V66W121 are nearly identical and consistent with a previous report on V66W136 [17]. It is notable that the V66W110 spectrum is very different from the V66W121/135 fragments spectra. The positive ellipticity around 270–285 nm in V66W121/135 is replaced by a negative signal in V66W110. The variation is likely caused by their alternative tertiary structure rather than by the extra amino acids in V66W121. Comparison of amino acid sequence shows that the aromatic residues of V66W110 differ

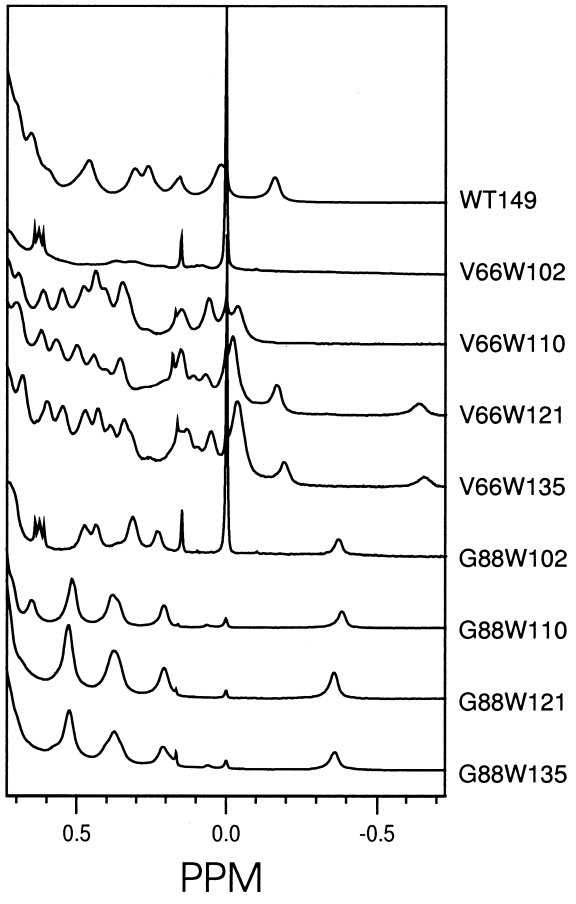

Fig. 4. ^{1}H-NMR spectra in upfield region for nuclease fragments in 50 mM d4-acetate buffer, 90%/10% H_2O/D_2O, pH 4.9. Note the disappearance of the two most upshifted resonances in V66W110 and the similarity of spectra for all G88W fragments.

from those of V66W121/135 in two tyrosine residues, Tyr-113 and Tyr-115. They are partially solvent exposed in the active cliff of native structure [18,19] and are expected to be more flexible in these C-terminal truncated fragments. Only aromatic residues in a fixed and asymmetrical environment give strong CD signals at the near-UV region. That there is no difference between the spectra of G88W110 and G88W121 also suggests that Tyr-113 and Tyr-115 in the fragments contribute very little to the signal. So, the distinct profiles of V66W110 and V66W121 reflect variations in their structure core.

Fig. 4 shows the 1D ^{1}H-NMR spectra in the upfield region. The upshifted resonance usually originates from the methyl protons which experience a ring current shielding effect from the neighboring aromatic side chain. The resonance position depends on the uniqueness of the three-dimensional structure and on the specific positions of the aromatic amino acids. The different positions of the tryptophans introduced to the V66W and G88W fragments should therefore significantly affect the upshifted signals. However, comparison among the fragments containing the same tryptophan substitution would be appropriate and meaningful. The NMR spectra of all fragments except V66W102 display extensive chemical shift dispersion, including upshifted resonances, indicative of substantial tertiary structure. The abundance of upshifted resonance in the structured V66W fragments is probably owning to the Trp-66 which is expected to be located in the interior of the β-barrel and has more residues in proximity. The disappearance of two most upshifted resonances at −0.65 and −0.15 ppm in V66W110 suggest alternative side chain packing compared with V66W121/135, which agrees well with the difference found in the near-UV CD spectra. As for the G88W fragments, all molecules, including the less stable G88W102, display very similar spectra in this region, indicating the same side chain packing in structure core.

The extent of solvent exposure of the tryptophan residues was examined by fluorescence emission and acrylamide quench. Table 1 gives the maxima of the fluorescence emission and the effective quench constants. As expected from the three-dimensional structure of SNase, if native-like β-barrel is maintained in the fragments, Trp-66 is deeply buried inside the β-barrel while Trp-88 is partially exposed to the solvent. Fluorescence data confirms this assumption and is consistent with a previous report on V66W136 and G88W136 [16,17]. The data also suggests a slight polar environment around Trp-66 in V66W110. It has an emission maximum at 330 nm which is shifted less to shorter wavelengths compared with V66W121/135 and it is more easily quenched. V66W102 exhibits intermediate λ_{max} at 339 nm between those of buried tryptophans in V66W110/121/135 and that of fully exposed tryptophan in the completely denatured molecule, suggesting that V66W102 is partially folded in aqueous solution.

3.3. Stability of fragments

GuHCl and thermal denaturation were used to

determine the thermodynamic parameters of these molecules. The GuHCl denaturation was completely reversible as shown by fluorescence spectra that were fully restored after 40-fold dilution of the unfolded protein in 2.5 M GuHCl (data not shown). The unfolding reactions were monitored separately by the tryptophan fluorescence at 325 nm as well as the far-UV CD at 222 nm, Fig. 5A,B. The fluorescence data indicated that all fragments except V66W102 demonstrated cooperative transition. However, sigmoidal change of CD signal was observed only in G88W110/121/135. The weak CD signal of the V66W fragments decreased nearly linearly as the GuHCl concentration increased (Fig. 5B), indicating the lack of cooperative and stable α-helix in the V66W fragments. The lack of sigmoidal CD curve in G88W102 may be in part due to its reduced α-helix content and stability.

Analysis of the unfolding curves with the two-state mechanism gave the unfolding free energy $\Delta G°H_2O$ and m values listed in Table 2. The estimated average error in the stability values is based on repeated analysis of different data sets for the same proteins under identical conditions. Compared with wild-type SNase, a much reduced stability and board transition zone (small m value) have been reported for V66W136 and G88W136 [16,17]. Our $\Delta G°H_2O$ and m values for V66W135 are 2.03 kcal/mol and 2.56 kcal/(mol·M), which are reasonably consistent with previously determined values of 2.40 kcal/mol and 2.73 kcal/(mol·M) [16] and 1.87 kcal/mol and 2.12 kcal/(mol·M) [17] for V66W136.

The thermal induced unfolding of fragments was also examined by fluorescence shown in Fig. 5C. The reversibility of the thermal unfolding, defined as the ratio of the fluorescence after and before the experiments, was around 85∼95%. It has been shown in SNase as well as in other proteins that thermal denaturation is not completely reversible, but depends

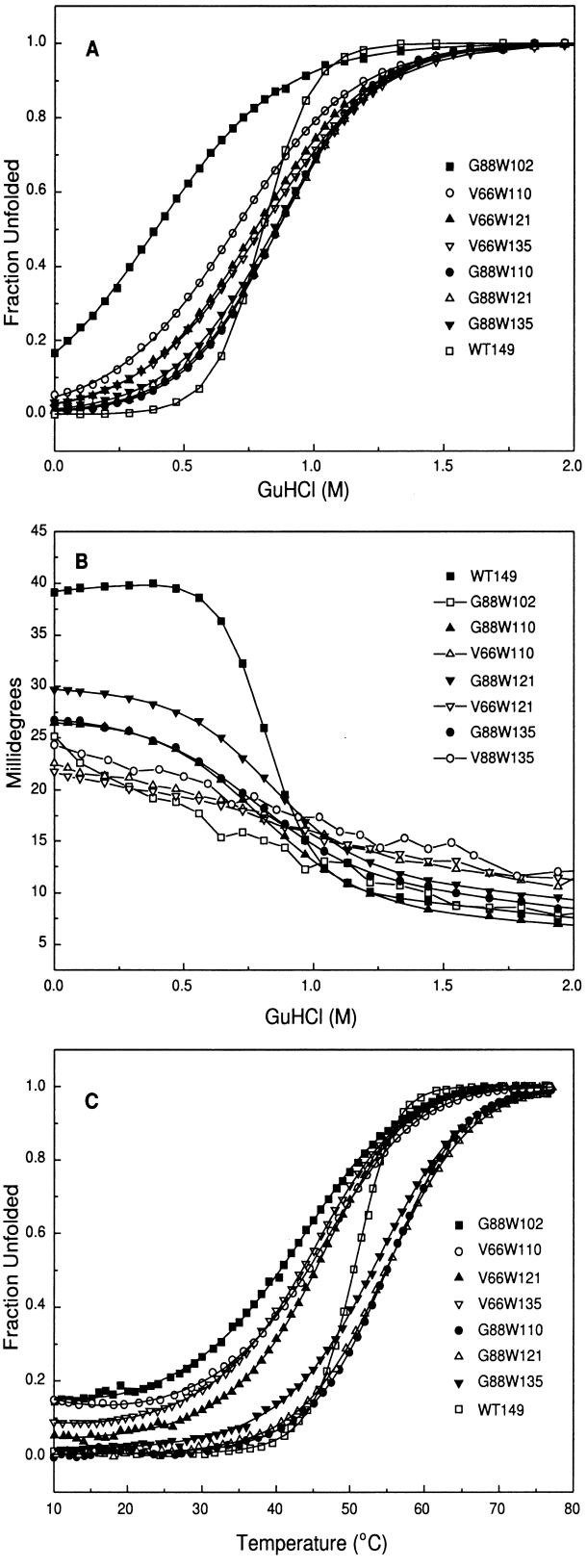

→

Fig. 5. Unfolding transitions for nuclease N-terminal fragments. Conditions as in Table 2. The solid lines are fits of the two-state model with the parameters in Table 2. (A) GuHCl unfolding monitored by fluorescence at 325 nm. (B) GuHCl unfolding monitored by CD at 222 nm. The data (open symbols) of the non-sigmoidal transition are connected directly. (C) Thermal unfolding transitions monitored by fluorescence at 325 nm.

Table 2
Thermodynamic parameters for GuHCl and thermal induced unfolding of staphylococcal nuclease fragments[a]

Fragments	GuHCl induced unfolding[b]				Thermal induced unfolding[c]		
	Fluorescence at 325 nm		CD at 222 nm				
	$\Delta G°H_2O$[d] (kcal/mol)	m[d] (kcal/(mol·M))	$\Delta G°H_2O$[e] (kcal/mol)	m[e] (kcal/(mol·M))	H_m (kcal/mol)	T_m (°C)	ΔC_p (kcal/(mol·K))
WT149	4.90	6.11	5.10	6.30	73.1 ± 0.4	50.4 ± 0.1	2.7 ± 0.1
V66W135	2.12	2.66	n.d.[h]	n.d.	27.5 ± 0.4	43.2 ± 0.3	0.9 ± 0.1
V66W121	2.07	2.76	n.d.	n.d.	32.5 ± 0.3	45.2 ± 0.1	1.0 ± 0.1
V66W110	1.75	2.57	n.d.	n.d.	25.5 ± 0.4	44.2 ± 0.2	0.9 ± 0.1
V66W102	−0.56[f]						
G88W135	2.56	3.06	2.22	2.92	35.6 ± 1.8	53.2 ± 0.3	0.8 ± 0.1
G88W121	2.55	3.03	2.78	3.37	35.4 ± 1.9	54.2 ± 0.6	0.7 ± 0.2
G88W110	2.74	3.23	2.20	2.85	41.4 ± 0.1	54.9 ± 0.1	0.9 ± 0.2
G88W102	0.94[g]	2.40[g]	n.d.	n.d.	22.0 ± 0.3[i]	40.9 ± 0.4[i]	0.8 ± 0.1[i]

[a]Protein concentrations were 3–5 μM in 10 mM Tris–HCl/pH 7.0/0.1 M NaCl and at 20°C (for GuHCl denaturation).
[b]Parameters obtained by fitting Eqs. 2 and 3 with all parameter floating or by sulfate renaturation.
[c]The thermal induced unfolding was monitored by fluorescence at 325 nm. Except for the case of G88W102, the parameters obtained by fitting Eqs. 4 and 5 with all parameters floating. Errors are based on two determinations.
[d]Estimated average error in $\Delta G°H_2O$ is less than ±0.1 kcal/mol and in m is less than ±0.1 kcal/(mol·M).
[e]Estimated average error in $\Delta G°H_2O$ is ±0.2 kcal/mol and in m is ±0.2 kcal/(mol·M).
[f]Values obtained by sulfate renaturation as described in [21]; the m value cannot be determined.
[g]Since the pretransition baseline of G88W102 is absent, it is assumed to have the same slope as G88W110 in the fitting routine.
[h]n.d., not determined because the CD data show no sigmoidal change with increasing GuHCl concentration, and no attempt was made to fit the 2-state model to data.
[i]Fitting done by fixed I_n and I_u taken from GuHCl denaturation (see Section 2).

strongly on the incubation duration at high temperature [20]. The apparent thermal unfolding parameters summarized in Table 2 were obtained by fitting the fluorescence data from thermal unfolding experiments to the two-state model. The results are the average of independent fitting outputs from the heating and cooling data sets. The values of enthalpy change $\Delta H°_{m,un}$ and heat capacity difference ΔC_p of the fragments are nearly half of these of WT149, indicating much less exposure of hydrophobic surface during the temperature unfolding reaction.

The stability of the tryptophan-containing fragment varies as a function of the polypeptide chain length. Both of the 1–102 fragments have much lower stability. There is great increase in stability when the C-terminal increases from 102 to 110 residues. Further elongation of the C-terminal does not significantly increase the stability. Obviously, residues 103–110 contribute most of the increased stability during the C-terminal elongation, 2.3 kcal/mol in V66W fragments and 1.8 kcal/mol in G88W fragments. The results demonstrate that residues 1–110 are necessary for the tryptophan-containing fragments to adopt a stable fold.

Compared with the V66W mutation, the G88W fragments seem more stable. Of the two shortest fragments, G88W102 has tertiary structure with marginal stability 0.94 kcal/mol, while V66W102 is unstable with no tertiary structure. G88W-110/121/135 also show slightly increased stability of 2.6 kcal/mol and the highest melting temperature of around 54°C, even higher than the 50°C for WT149.

4. Discussion

An intermediate state has been found in the folding pathway of SNase. It consists of native-like β-barrel and largely disordered α-helix [7–11]. The structure of the intermediate state can be stabilized by many mutations, such as V66L, V66W, G88V, G88W [7,8]. These hydrophobic substitutions at position 66 or 88 were proposed to strengthen the hydrophobic core in the β-barrel [22]. In the character-

ization of the intermediate state properties, a C-terminal truncated 1–136 fragment of SNase appears as an appropriate model and has been extensively studied in the non-denaturing condition [12–17]. The 1–136 fragment lost most of the helical secondary structure while remaining compact in the absence of any added denaturant. It retained a large fraction of enzymatic activity and was able to refold to native-like state under the presence of two SNase ligands Ca^{2+} and pdTp as revealed by CD spectroscopy, NMR, and small-angle X-ray scattering [12,13]. The results of conformation-dependent chemical cleavage experiments suggested that the polypeptide backbone spanning the β-barrel–helix 1–helix 2 system follows a dynamic, but largely native-like, topology, while helix 3 and its connecting loop to helix 2 are disordered [14]. In the more structured G88V136, the residues 99–136 were found to be flexible while the β-barrel was closely native-like [15]. Furthermore, the break down of the V66W136 fragment accurately describes the second half transition of the intermediate to the fully unfolded state in a three-state unfolding model of V66W149 [16,17]. In this study, V66W and G88W fragments are used as intermediate analogues to probe the possible interactions of the β-barrel with the C-terminal tail (103–135) and to identify the minimal structure core in the tryptophan-containing fragments.

Tryptophan substitutions at 66 and 88 positions influence differently the conformation and stability of the fragments. G88W fragments are more helical and more stable possibly caused by the different disturbances created by the tryptophan mutations. The bulk indole ring of Trp-66 in the β-barrel interior of the V66W fragments is more likely to disturb the β-barrel structure and stability. The increased *m* value in the G88W fragments, which is commonly regarded as proportional to the difference between the denaturant accessible surface in the folded and unfolded states, is probably due to the well-formed α-helix that decreases the denaturant accessible surface.

Spectroscopic properties indicate that these fragments are all partially folded, yet do not belong to the molten globule state [3]. Neither fragment binds 8-anilinonaphthalene-1-sulfonate (ANS), a dye that binds to a hydrophobic patch which is characteristic of the molten globule state (data not shown). Tertiary structures and cooperative unfolding transitions in the fragments also argue against the molten globule state.

The least structured fragment, V66W102, has no tertiary structure as indicated by its near-zero ellipticity in the near-UV range and little dispersion of the ^{1}H-NMR spectrum. Nevertheless, V66W102 may not be a completely random coil in aqueous solution as suggested by its fluorescence emission maximum around 339 nm and its residual far-UV CD signal. Renaturation by ammonium sulfate returned V66W102 to a state with a fluorescence emission maximum at 330 nm and a cooperative unfolding transition (data not shown). It is estimated that 30% of V66W102 molecule is structured in solution.

A significant increase in the stability of these tryptophan-containing fragments occurs when the C-terminal grows from 102 to 110 residue. In our previous studies on wild-type N-terminal fragments (with no tryptophan substitution), sheet-like structure increases from 6.5 to 17.7% between WT102 and WT110, as revealed by Fourier transform infrared spectroscopy [25], suggesting the interactions with segment 103–110 favor the formation of β-sheet structure. However, neither wild-type N-terminal fragment has a stable structure core which prevents quantitative estimates of the stability contributed by this segment. The stability gain provided by residues 103–110 approximates 2 kcal/mol in the tryptophan-containing fragments. Residues 103–110 constitute the second helix (99–106) in the native structure of SNase (Fig. 1). The second helix is fairly autonomous structural element which persists in a denatured fragment, Δ131Δ [23]. Moreover, an isolated polypeptide containing the helix 2 sequence was estimated to have 30% α-helix conformation in aqueous solution [24]. The high intrinsic propensity for helical conformation of this segment may account for its active role in maintaining the structure core in fragments.

Residues after 110 contribute little to the stability of the structure core. However, V66W110 and V66W121 have noticeable differences in their near-UV spectrum and upfield NMR signals. Fluorescence data also suggest more polar environment around tryptophan in V66W110. These results support the conclusion that V66W110 has an alternative tertiary structure with V66W121. Our preliminary

NMR characterization found that the ^{1}H-^{15}N heteronuclear correlation spectrum of V66W121 consists of two sets of peak with the minor set coinciding with that of V66W110 (Ye K. and Wang J. preliminary observation), suggesting that V66W121 adopts two conformations in solution. The minor conformation is identical to that of V66W110 and transforms to the major one over a slow NMR time-scale ($\ll 10^3$ s^{-1}). It is unclear about the structural difference of two conformations and the details of the conformational transforming. Extra interactions with residues 111–121 in V66W121 seem to be the apparent cause of the conformational transformation. Residues 111–121, which form a loop linking helix 2 and 3 in the native state of SNase, have been found to be disordered in WT136 and G88V136 [14,15]. However, our results demonstrate that segment 111–121 may not be completely random coil and may participate in the long-range interactions with the formed structure in V66W121. Such significant effects of residue 111–121 were not observed in the G88W fragments, possibly because the strong stabilizing effects of G88W mutation prevent the detection of other minor interactions with the β-barrel.

V66W110 and G88W110 were found to be minimally stable module in the tryptophan-containing fragments studied here. Another smaller fragment containing the 1–103 residues and G88V+V66L double mutations also showed stable and cooperative β-barrel [22]. These isolated stable subdomains clearly reflect the modular nature of SNase. In a previous kinetic folding study of SNase, the location of the usual structure reporters in SNase, such as the α-helices or the single tryptophan at the position 140 being outside the β-subdomain prevents direct characterization of the kinetic phase involving the rapid formation of β-barrel [11]. The V66W110 and G88W110 with a single fluorescence reporter in the β-barrel are expected to be suitable for kinetic folding studies of the isolated β-subdomain.

The N-terminal fragments have been proposed to have similar structural characteristics as the nascent polypeptide when it is synthesized from the N-terminal in ribosome [1]. Examination of the development of the polypeptide chain structure as the C-terminal increases would help to understand how the nascent polypeptide folds in vivo [1]. Studies on the N-terminal fragments of chymotrypsin inhibitor 2, which approaches the minimum structure module, showed that its folding process is concerted and highly cooperative [35]. However, studies of N-terminal fragments of SNase suggested that its folding behavior, which has an intrinsic multiple modular nature, is hierarchical with elements of structure building up sequentially [25–27]. The results obtained here from two tryptophan mutants dissect the extent of the long-range interaction in the partially folded fragments.

Acknowledgements

This research was supported in part by the Pandeng Project of the National Commission for Science and Technology and by Grant 39570171 from the China Natural Science Foundation.

References

[1] C.L. Tsou, Biochemistry 27 (1988) 1809–1812.
[2] A.L. Fink, Annu. Rev. Biophys. Biomol. Struct. 24 (1995) 495–522.
[3] K. Kuwajima, Proteins: Struct. Funct. Genet. 6 (1989) 87–103.
[4] P.L. Privalov, J. Mol. Biol. 258 (1996) 707–725.
[5] M. Llinás, S. Marqusee, Protein Sci. 7 (1998) 96–104.
[6] M.S. Kay, R.L. Baldwin, Nat. Struct. Biol. 3 (1996) 439–445.
[7] J.H. Carra, E.A. Anderson, P.L. Privalov, Biochemistry 33 (1994) 10842–10850.
[8] J.H. Carra, P.L. Privalov, Biochemistry 34 (1995) 2034–2041.
[9] D. Xie, R. Fox, E. Freire, Protein Sci. 3 (1994) 2175–2184.
[10] M.D. Jacobs, R.O. Fox, Proc. Natl. Acad. Sci. USA 91 (1994) 449–453.
[11] W.F. Walkenhorst, S.M. Green, H. Roder, Biochemistry 36 (1997) 5795–5805.
[12] D. Shortle, A.K. Meeker, Biochemistry 28 (1989) 936–944.
[13] J.M. Flanagan, M. Kataoka, D. Shortle, D.M. Engelman, Proc. Natl. Acad. Sci. USA 89 (1992) 748–752.
[14] M.R. Ermacora, D.W. Ledman, R.O. Fox, Nat. Struct. Biol. 3 (1996) 59–66.
[15] D. Shortle, C. Abeygunawardana, Structure 1 (1993) 121–134.
[16] A.G. Gittis, W.E. Stites, E.E. Lattman, J. Mol. Biol. 232 (1993) 718–724.
[17] M.R. Eftink, R.M. Ionescu, G.D. Ramsay, C.Y. Wong, J.Q. Wu, A.H. Maki, Biochemistry 35 (1996) 8084–8094.

[18] T.R. Hynes, R.O. Fox, Proteins: Struct. Funct. Genet. 10 (1991) 92–105.
[19] J. Wang, D.M. Truckses, F. Abildgaard, Z. Dzakula, E. Zolnai, J.L. Markley, J. Biomol. NMR 10 (1997) 143–164.
[20] D. Shortle, A.K. Meeker, E. Freire, Biochemistry 27 (1988) 4761–4768.
[21] D. Shortle, W.E. Stites, A.K. Meeker, Biochemistry 29 (1990) 8033–8041.
[22] A.T. Alexandrescu, A. Gittis, C. Abeygunawardana, D. Shortle, J. Mol. Biol. 250 (1995) 134–143.
[23] A.T. Alexandrescu, C. Abeygunawardana, D. Shortle, Biochemistry 33 (1994) 1063–1072.
[24] Y. Wang, D. Shortle, Folding Design 2 (1997) 93–100.
[25] G.Z. Jing, B. Zhou, L. Xie, L.J. Liu, Z.G. Liu, Biochim. Biophys. Acta 1250 (1995) 189–196.
[26] B. Zhou, G.Z. Jing, J. Biochem. 120 (1996) 881–888.
[27] K. Tian, B. Zhou, F. Geng, G. Jing, Int. J. Biol. Macromol. 23 (1998) 199–206.
[28] F.W. Studier, A.H. Rosenberg, J.J. Dunn, J.W. Dubendorf, Methods Enzymol. 185 (1990) 60–89.
[29] J. Sambrook, T. Maniatis, E.F. Fritsch, Molecular Cloning: A Laboratory Manual, Cold Spring Harbor Laboratory Press, Cold Spring Harbor, NY, 1989.
[30] S.C. Gill, P.H. von Hippel, Anal. Biochem. 182 (1989) 319–326.
[31] M.R. Eftink, C.A. Ghiron, Anal. Biochem. 114 (1981) 199–227.
[32] M. Piotto, V. Saudek, V. Sklenar, J. Biomol. NMR 2 (1992) 661–665.
[33] M.M. Santoro, D.W. Bolen, Biochemistry 27 (1988) 8063–8068.
[34] N. Sreerama, R.W. Woody, Anal. Biochem. 209 (1993) 32–44.
[35] G. De Prat Gay, J. Ruiz-Sanz, J.L. Neira, L.S. Itzhaki, A.R. Fersht, Proc. Natl. Acad. Sci. USA 92 (1995) 3683–3686.
[36] P.J. Kraulis, J. Appl. Crystallogr. 24 (1991) 946–959.